Available online at www.sciencedirect.com
ScienceDirect
Journal of Nuclear Materials 375 (2008) 224–228
journal of nuclear materials
www.elsevier.com/locate/jnucmat

Blister formation on tungsten damaged by high energy particle irradiation

M. Fukumoto [a,*], Y. Ohtsuka [a], Y. Ueda [a], M. Taniguchi [b], M. Kashiwagi [b], T. Inoue [b], K. Sakamoto [b]

[a] Graduate School of Engineering, Osaka University, 2-1 Yamadaoka, Suita, Osaka 565-0871, Japan
[b] Japan Atomic Energy Agency, 801-1 Mukouyama, Naka, Ibaraki 331-0193, Japan

Received 10 April 2007; accepted 26 November 2007

Abstract

In order to investigate the effect of radiation damage on hydrogen behavior in tungsten, tungsten samples with radiation damage of up to 3.5 dpa were irradiated by a mixed hydrogen–carbon ion beam. The radiation damage was produced with 700 keV negative hydrogen ion beam irradiation. The number density of blisters produced by the mixed ion beam irradiation decreased with increasing radiation damage. This was especially observed for blisters with diameters of 20 μm or less. This result showed that radiation damage produced by high-energy particle irradiation suppresses blister formation on tungsten surfaces.

PACS: 28.52.Fa; 52.40.Hf; 61.80.Jh

1. Introduction

Tungsten is one of the candidate materials for plasma facing components (PFCs) of future fusion devices because of its high melting temperature, low sputtering yield, and low solubility for hydrogen. Studies of hydrogen isotope ion irradiation of tungsten have been performed with ion beam devices and plasma simulators [1–3]. These studies showed blistering occurring on the tungsten surface due to trapping of irradiated hydrogen isotopes at grain boundaries. In the case of adding carbon ions of more than 0.3% to a hydrogen ion beam, blister formation on the tungsten surface was enhanced [4]. These studies were performed for tungsten with no prior radiation damage.

In D–T fusion reactors, fast neutrons generated by D–T nuclear reactions will bombard plasma facing materials (PFMs) and produce radiation damage. Therefore, the effects of radiation damage in tungsten on hydrogen isotope behavior and embrittlement need to be studied. In order to simulate the effects of fast neutron damage, radiation damage produced by high-energy ions has been used in some previous studies [5–8]. In these studies deuterium retention and distribution in some materials (nickel, vanadium, copper, and tungsten) damaged by high-energy ion beam were investigated by exposing to pure deuterium plasma. These studies showed that post-irradiated deuterium was trapped at radiation damage produced by high-energy ion beam pre-irradiation. Oliver et al. also reported that radiation induced defects in tungsten produced by 800 MeV proton irradiation were removed by annealing at 1273 K for 6 h [8]. However, blister formation and embrittlement of tungsten damaged by high-energy particle irradiation are still not fully understood.

In this study, effect of radiation damage on blistering was investigated. Radiation damage was produced by a high-energy negative hydrogen ion beam. In order to form blister even at low fluences, a high flux mixed hydrogen and carbon ion beam was used in this study. From the previous

* Corresponding author. Tel.: +81 6 6877 5111x3309; fax: +81 6 6879 7867.
E-mail address: fukumoto@st.eie.eng.osaka-u.ac.jp (M. Fukumoto).

0022-3115/$ - see front matter © 2008 Elsevier B.V. All rights reserved.
doi:10.1016/j.jnucmat.2007.11.005

study, blistering was promoted by the mixed hydrogen and carbon ion beam irradiation while this was not observed by a hydrogen ion beam irradiation. This is due to reduction of hydrogen recombination rate on the WC surface formed by mixed hydrogen and carbon ion beam irradiation and decrease of hydrogen desorption. Details were discussed elsewhere [4].

2. Recovery of radiation damage of tungsten

The recovery of tungsten defects induced by neutron irradiation ($E_n > 1$ MeV) at reactor ambient temperature (about 373 K) have been studied via isochronal annealing resistivity recovery and field ion microscopy (FIM) [9–14]. These studies showed that there are three principal recovery stages above 343 K. The Stage III recovery, the intermediate one, and the Stage IV recovery occurred at $\sim 0.15T_m$, $\sim 0.22T_m$, and $\sim 0.31T_m$, respectively, where T_m is the melting temperature of tungsten in K. For the Stage III recovery region Attardo et al. concluded that the self-interstitials produced by neutron irradiation migrate and recombine with vacancies [11]. The intermediate recovery region occurring at $\sim 0.22T_m$ is considered to be due to divacancies, impurities, impurity defect complexes, or interstitials which escaped from shallow impurity traps [12]. The Stage IV recovery is attributed to migration of the excess vacancies [13,14]. FIM studies by Jeannotte et al. indicated that irradiation-produced vacancies are the effective sinks in the vacancy annihilation process [14].

3. Experimental

In this study, polycrystalline tungsten samples with a purity of 99.99 at.% obtained from Allied Material Corporation were used. These samples were hot-rolled and annealed at 1173 K for 0.5 h in a hydrogen atmosphere to relieve internal stresses. The samples were cut into pieces with dimension of 20, 10, and 1 mm thickness. These surfaces were mechanically mirror-polished to a surface roughness of less than 0.1 μm.

Radiation damage in the tungsten samples was produced by a high-energy negative hydrogen ion beam in the MeV Test Facility at the Japan Atomic Energy Agency. Details of this facility were reported elsewhere [15]. Tungsten samples were fixed on a sample holder made of copper. Carbon sheets were inserted between the sample holder and the tungsten samples in order to increase heat conduction and to reduce temperature increases during high-energy negative hydrogen ion beam irradiation. The cesium oven in the ion source was heated to reduce the oxygen impurity in the vacuum chamber. The beam energy and fluence were 700 keV and $\sim 1.6 \times 10^{22}$ H^-/m^2, respectively. According to studies of isochronal resistivity recovery by Keys et al. the radiation damage in tungsten was recovered rapidly above 473 K [10]. Therefore, in the present study the high-energy negative hydrogen ion beam pre-irradiation was performed repeatedly for 0.2–1.0 s every 60 s to limit the highest surface temperature to below 473 K.

Following damage creation, the samples were post-irradiated with a high flux ion beam of mixed hydrogen and carbon in the HiFIT device [16,17]. The hydrogen beam energy, flux, fluence, and sample temperature were 1.0 keV, $\sim 2.2 \times 10^{20}$ H^+/m^2 s, $\sim 7.5 \times 10^{24}$ H^+/m^2, and 473 K, respectively. By using this device, hydrogen and carbon ions were simultaneously irradiated onto the sample with no mass selection. The hydrogen ions were produced by an electron cyclotron resonance (ECR) discharge. Carbon ions were added by placing carbon plates in the hydrogen ion source chamber. Carbon ion concentration in the irradiation beam was ~0.8%. Therefore, the effect of implanted carbon ions on blister formation is the same for all tungsten samples, since same fractions of carbon ions were irradiated to all tungsten samples. The hydrogen ion species in the beam were H_3^+ (~65%), H_2^+ (~10%), and H^+ (~25%). The respective energies per hydrogen atom were 0.3, 0.5, and 1.0 keV when the ion acceleration voltage was set to 1.0 kV. Since the carbon ions in the beam were contained in CH_x^+ and $C_2H_x^+$ molecular ions, the energy of the carbon atoms was roughly 0.5 and 1.0 keV. The oxygen impurity in the beam was less than 0.05%. Details of the mass spectrum of the mixed H^+–C^+ ion beam were reported previously [17,18].

The tungsten samples were attached to a copper plate, in which an alumel–chromel thermocouple was embedded to measure the sample temperature. The ion beam irradiation area was defined by a 5 mm diameter aperture just in front of the samples. The samples were heated by an infrared heater from the backside.

Surface morphologies of the post-irradiated samples were observed by a scanning electron microscope (SEM). The depth profile of atomic composition was measured by X-ray photoelectron spectroscopy (XPS; AXIS 165,

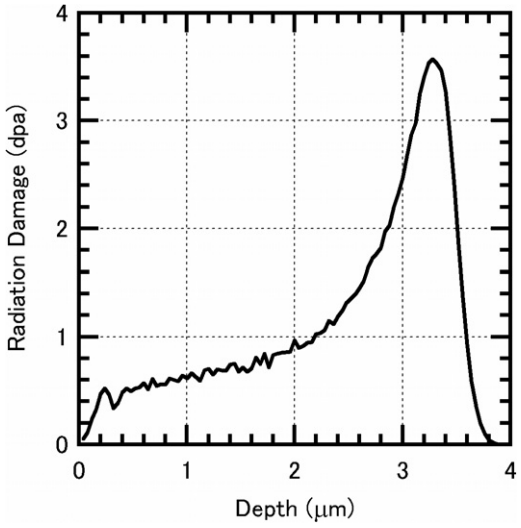

Fig. 1. Depth profile of radiation damage (vacancy production per one lattice atom) calculated by TRIM-88 [19] for a negative hydrogen ion beam of 700 keV energy and of $\sim 1.6 \times 10^{22}$ H^-/m^2 fluence.

Kratos Co.) with the MgKα line (energy: 1253.6 eV). Prior to performing XPS, the samples were exposed to air. Depth profiles were obtained by 3 keV Ar beam etching. The depth of the etched area was measured by a surface profilometer (Dektak3, Veeco Co.). The cross section of the blisters formed on the tungsten surface was observed by focused ion beam (FIB) devises with 30 keV gallium ion beam. With these devises, we fabricated the cross section of the blisters and obtained secondary electron images from the cross sections.

4. Results and discussion

The depth profile of the radiation damage calculated by TRIM-88 [19] is shown in Fig. 1. The calculation was based on the experimental parameters of the irradiating high-energy negative hydrogen ion beam (i.e., 700 keV energy and $\sim 1.6 \times 10^{22}$ H^-/m^2 fluence). As shown in Fig. 1, the radiation damage increases with depth until it reaches a maximum around 3.3 μm. The maximum radiation damage was about 3.5 dpa. In this paper, radiation damage for the tungsten samples was defined as that at 3.3 μm in depth.

Three samples with radiation damage of 0, ~0.3, and ~3.5 dpa were post-irradiated with a low-energy H^+–C^+ beam. The 0 dpa means no pre-irradiation by the 700 keV negative hydrogen ion beam. Fig. 2 shows a SEM photograph of the samples post-irradiated with low-energy hydrogen and carbon ions. The blister size distribution with radiation damage as a parameter is shown in Fig. 3. Sum of the number density of blisters with diameters 1–100 μm for the 0 dpa sample was about 3500 mm^{-2} and it decreased with increasing radiation damage. In the cases of ~0.3 and ~3.5 dpa, sum of the number densities of blisters with diameters 1–100 μm were about 370 and 100 mm^{-2}, respectively. For the damaged samples, the main decrease was observed for blisters with diameters of 20 μm or less; the number of blisters with diameters of 20 μm or more was not significantly changed.

Fig. 4 shows carbon and oxygen depth profiles of the atomic composition of the post-irradiated samples measured by XPS for (a) 0 dpa and (b) ~3.5 dpa damage. The binding energies associated with compounds of C, O, and W are as follows; Graphite: 284.5 eV and WC: 283.2 eV; O_2: 532.0 eV and WO_3: 530.5 eV, and tungsten: 33.4 and 31.4 eV. Carbon atoms with graphitic bonds and WC co-existed from the top surface to a depth of ~2 nm for both samples. At ~2 nm depth, most of the carbon bonded with tungsten to form WC. The carbon atom concentration in WC decreased with depth, reaching negligible levels at about 10–15 nm. About 5–10 at.% oxygen existed over the measurement ranges. The oxygen atoms could have originated from the residual gases in the XPS device [20]. From the XPS profiles, no significant differ-

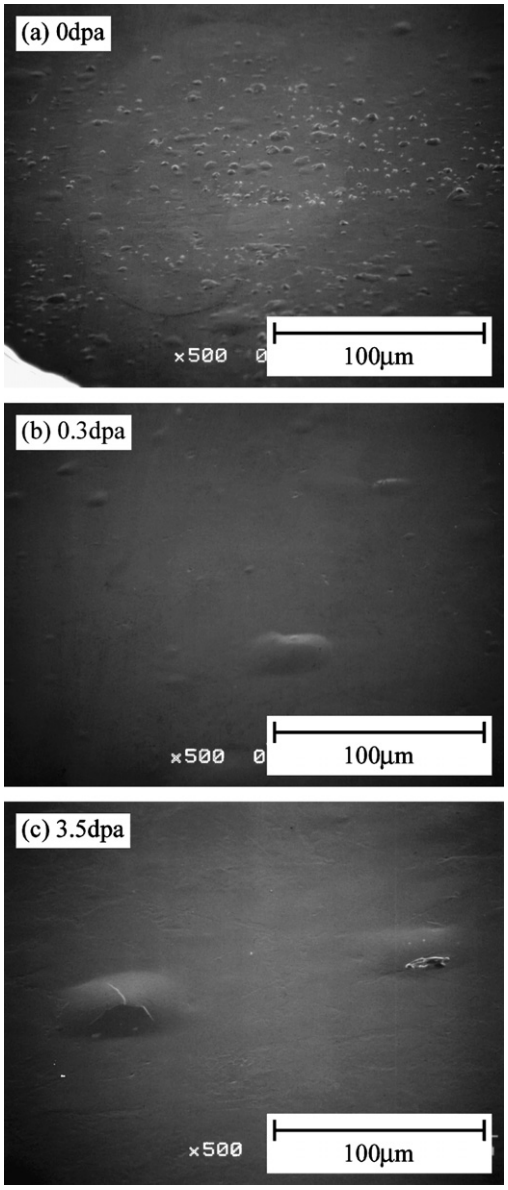

Fig. 2. SEM photograph of the tungsten samples with (a) 0 dpa, (b) ~0.3 dpa, and (c) ~3.5 dpa damage after mixed H^+–C^+ ion beam irradiation.

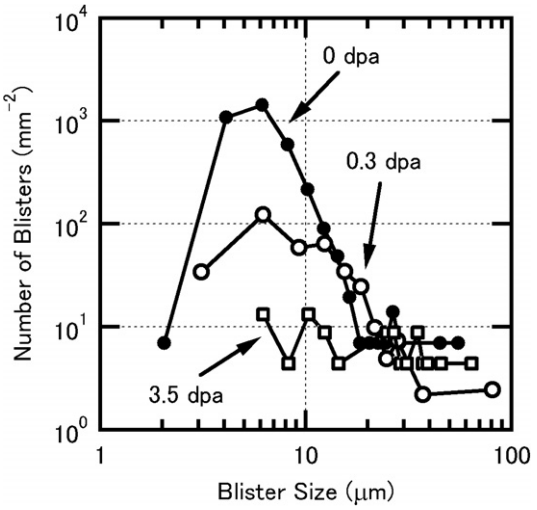

Fig. 3. Blister size distribution with radiation damage as parameters.

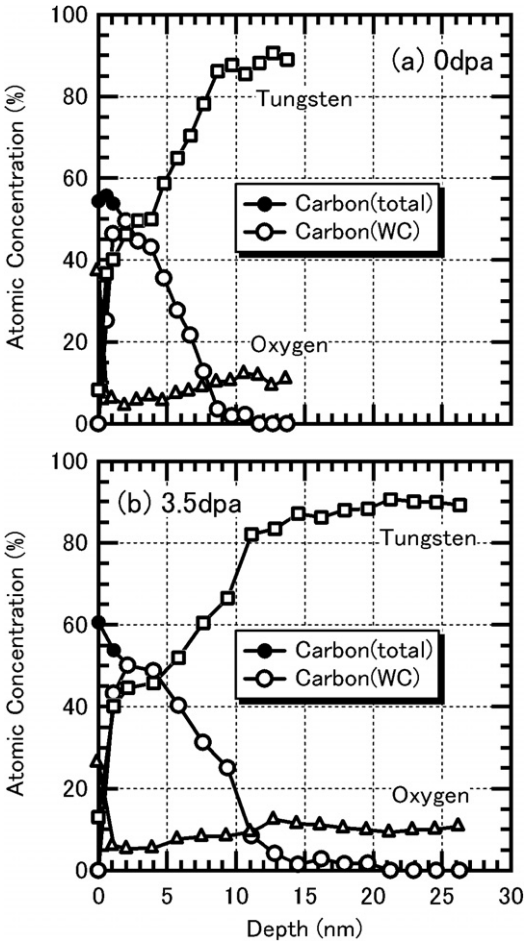

Fig. 4. Depth profile of tungsten, carbon, and oxygen for (a) 0 dpa and (b) ~3.5 dpa samples after mixed H^+–C^+ ion beam irradiation.

ences in atomic composition are seen for the tungsten samples. Therefore, the radiation damage in the tungsten did not affect the distribution of the implanted carbon.

Fig. 5 shows a cross sectional view of a blister formed by mixed H^+–C^+ beam irradiation in the 0 dpa sample, as observed by FIB. Grains with different crystal orientation are shown by different brightness. The area enclosed with a broken line contains a blister gap at a depth of 1–2 μm

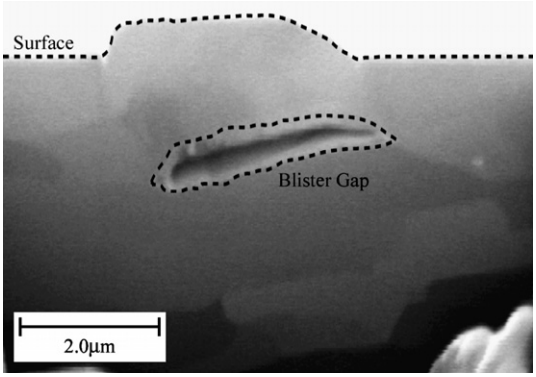

Fig. 5. Photograph obtained by FIB of the tungsten sample with 0 dpa after mixed H^+–C^+ ion beam irradiation. The broken line on the top shows the surface of the sample.

at grain boundaries. The diameter of this blister was ~5.5 μm; this location is deeper than the range of the 700 keV negative hydrogen ion beam (3.3 μm).

Depth profiles of deuterium in materials damaged with high-energy hydrogen ion beam irradiation showed that the incident deuterium is trapped at radiation-induced defects such as vacancies and interstitials in a damaged material [5]. In our study, it could be considered that the post-irradiated hydrogen was also trapped at radiation-induced defects produced by the 700 keV negative hydrogen ion beam pre-irradiation.

We estimated the depth of blister gaps in blisters whose diameter was 20 μm or more, which did not change with radiation damage. For D^+ irradiation of Haasz et al. showed that a large blister with a diameter of approximately 100 μm (accurate diameter was not shown) had a blister gap at a depth of ~10 μm [2]. A cross-sectional view of a blister formed on tungsten irradiated with a mixed H^+–C^+ ion beam at 653 K is shown in Fig. 6; a blister gap at a depth of ~5 μm is seen for a blister with ~25 μm diameter. The relationship between blister diameter and the depth of gaps is shown in Fig. 7; the gray color represents the radiation-damaged region. As shown in Fig. 7 the depth of blister gaps increases with blister diameter, and the ratio between the depth of gaps and the blister

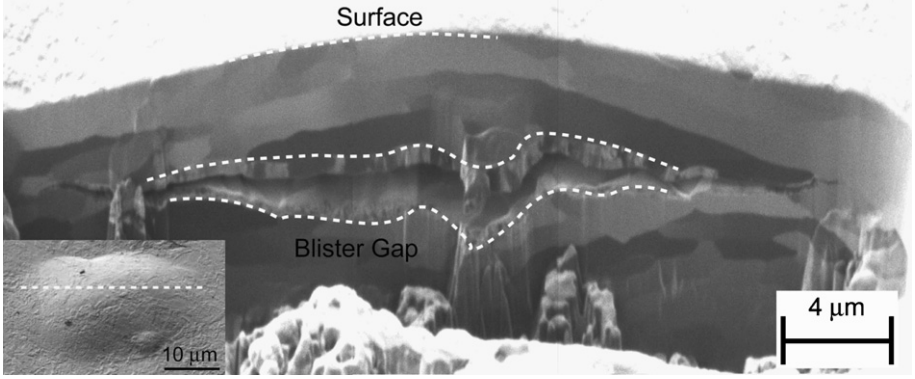

Fig. 6. Photograph obtained by FIB of a blister gap formed by irradiation of tungsten with a mixed H^+–C^+ ion beam at 653 K.

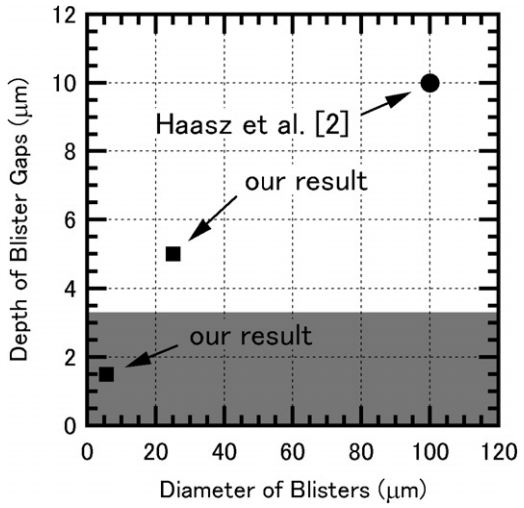

Fig. 7. Relationship between blister diameter and the depth of gap formation. The gray colored band represents the radiation-damaged region produced by the 700 keV negative hydrogen ion beam pre-irradiation. Data taken from Ref. [2] are also shown.

diameter is in the range 0.1–0.2. According to this ratio, the depth of the blister gaps for large blisters with diameters >20 μm in the present study is expected to be more than 4 μm, with the implication that blister gaps in the damaged samples could be formed beyond the radiation-damaged region.

Since the post-irradiated hydrogen is trapped not only at grain boundaries but also at radiation-induced defects such as vacancies and interstitials, trapping of the post-irradiated hydrogen at grain boundaries might be lower for the damaged samples. Therefore, the formation of blister with diameters of 20 μm or less, whose blister gaps would have existed at depths of less than 4 μm, was suppressed by the 700 keV negative hydrogen ion beam pre-irradiation. On the other hand, in the case of blisters with more than 20 μm diameter, changes in blister distribution were small, since radiation damage was not produced at the depth of the blister gaps.

5. Conclusion

In this study, effect of radiation damage on hydrogen behavior in tungsten was investigated in terms of blister formation and its characteristics. Radiation damage was produced by the 700 keV negative hydrogen ion beam.

The number of blisters with diameter of 20 μm or less was decreased with increasing radiation damage. These blisters had blister gaps with less than 4 μm in depth in agreement with the radiation-damaged region produced by 700 keV negative hydrogen ion beam irradiation. Therefore, it can be concluded that blister gaps were not formed in the radiation-damaged region. Since the post-implanted hydrogen was trapped not only at grain boundaries but also at radiation damage, the hydrogen retained at grain boundaries could be decreased.

From these observations, radiation damage produced by high-energy particles (ions and neutrons) could suppress the blister formation of tungsten.

Acknowledgments

The authors are very grateful to Professor Kurishita in Tohoku University and Dr Sano in Osaka University for fabrication and observation of cross section of post-irradiated tungsten samples by FIB.

References

[1] R.A. Causey, J. Nucl. Mater. 300 (2002) 91.
[2] A.A. Haasz, M. Poon, J.W. Davis, J. Nucl. Mater. 266&269 (1999) 520.
[3] W. Wang, J. Roth, S. Lindig, C.H. Wu, J. Nucl. Mater. 299 (2001) 124.
[4] Y. Ueda, T. Shimada, M. Nishikawa, Nucl. Fusion 44 (2004) 62.
[5] I. Takagi, H. Fujita, K. Yoshida, K. Shin, K. Higashi, J. Nucl. Mater. 212&215 (1994) 1411.
[6] I. Takagi, N. Matsubara, M. Akiyoshi, K. Moritani, T. Sasaki, H. Moriyama, Nucl. Instrum. and Meth. B 232 (2005) 327.
[7] I. Takagi, M. Akiyoshi, N. Matsubara, K. Moritani, H. Moriyama, Fusion Eng. Design 81 (2006) 785.
[8] B.M. Oliver, R.A. Causey, S.A. Maloy, J. Nucl. Mater. 329&333 (2004) 977.
[9] L.K. Keys, J.P. Smith, J. Moteff, Phys. Rev. 176 (1968) 851.
[10] L.K. Keys, J. Moteff, J. Nucl. Mater. 34 (1970) 260.
[11] M.J. Attardo, J.M. Galligan, J.G.Y. Chow, Phys. Rev. Lett. 19 (1967) 73.
[12] J. Moteff, J.P. Smith, ASTM, STP-380, 1965. p. 171.
[13] M.J. Attardo, J.M. Galligan, Phys. Status Solidi 16 (1966) 449.
[14] D.M. Jeannotte, J.M. Galligan, Phys. Rev. Lett. 19 (1967) 232.
[15] T. Inoue, M. Taniguchi, T. Morishita, M. Dairaku, M. Hanada, T. Imai, M. Kashiwagi, K. Sakamoto, T. Seki, K. Watanabe, Nucl. Fusion 45 (2005) 790.
[16] T. Shimada, Y. Ueda, A. Sagara, M. Nishikawa, Rev. Sci. Instrum. 73 (2002) 1741.
[17] Y. Ueda, H. Kikuchi, T. Shimada, A. Sagara, B. Kyoh, M. Nishikawa, Fusion Eng. Design 61&62 (2002) 947.
[18] T. Shimada, H. Kikuchi, Y. Ueda, A. Sagara, M. Nishikawa, J. Nucl. Mater. 313&316 (2003) 204.
[19] W. Eckstein, Computer Simulation of Ion-Solid InteractionSpringer Series in Material Science, vol. 10, Springer, Berlin, 1991.
[20] Y. Ueda, M. Fukumoto, I. Sawamura, D. Sakizono, T. Shimada, M. Nishikawa, Fusion Eng. Design 81 (2006) 233.